Seismic Response Analysis of a Concrete Filled Steel Tubular (CFST) Arch Bridge

K. Bi & H. Hao
University of Western Australia, Australia

W. Ren
Hefei University of Technology, China

SUMMARY:
This paper studies the seismic responses of Yeshan River Bridge, a concrete filled steel tubular (CFST) arch bridge, to multi-component spatially varying ground motions. The three-dimensional (3D) finite element model of the CFST arch bridge is developed with consideration of the material and geometric nonlinearities of the arch ribs. The spatial variation of ground motions associated with wave passage, coherency loss and local site effects is considered. The influences of ground motion spatial variations and varying site conditions on the seismic responses of the CFST arch bridge are analysed.

Keywords: CFST arch bridge, nonlinear seismic response, spatial variation, local site effect

1. INTRODUCTION

The construction of concrete filled steel tubular (CFST) arch bridges has become widespread all over the world and especially in China in recent decades because of many inherent advantages of this bridge type. For example, the infilled concrete prevents local buckling of the steel tube while the steel tube confines the concrete to resist tension, bending moment and shear force, thus the composite structural action of the infilled concrete and the steel tube improves the member's load-carrying capacity. Moreover, the tube can act as a framework for the concrete during the construction of the bridge, which saves a majority of construction cost (Wu *et al*. 2006). The first CFST arch bridge in China was completed in 1990. Since then, more than 300 CFST arch bridges have been built or under construction.

Owing to the improved load-carrying capacity of CFST arch bridge, the span length of this kind of bridge can be longer than the conventional concrete arch bridge or steel arch bridge. For example, the span of Wuxia Yangtze River Bridge in China reaches as long as 460m. It is well known that for these long span structures, the ground motions at different supports during an earthquake inevitably vary, which is known as the ground motion spatial variations. Many reasons result in ground motion spatial variations, these include (1) the difference in the arrival times of seismic waves at different supports, denoted as the wave passage effect; (2) the coherency loss effect owing to the reflections and refractions of the waves in the heterogeneous media of the ground; and (3) the local site effect due to different local soil conditions (Der Kiureghian 1996).

Many researchers have studied the influence of ground motion spatial variations on the seismic response of arch structures (Hao 1993, 1995; *Harichandran* et al. 1996; Zanardo *et al*. 2004; *Su et al*. 2007; Bai *et al*. 2010). They concluded that ground motion spatial variations have great influence on the structural responses, and in cases might even govern the responses. However, most previous studies of dynamic analysis of arches mainly focused on the relatively simple structural types based primarily on 2D models, comprehensive studies of CFST arch bridges based on 3D models are relatively limited. Wu *et al*. (2006) performed a nonlinear seismic analysis of the Second Saikai Bridge (which is the first CFST arch bridge in Japan) by using the strong ground motions observed in the Hyogo-ken Nanbu Earthquake in Japan. The nonlinear seismic characteristics and seismic safety of

this bridge were examined in detail by subjecting the bridge to earthquakes in the out-of-plane direction, longitudinal direction and combined out-of-plane and longitudinal directions. However, it should be noted that the ground motions at different supports of the bridge are assumed to be the same and the influence of ground motion spatial variations are not considered in the paper. This assumption may lead to inaccurate prediction of seismic responses based on previous studies.

The present paper studies the nonlinear seismic responses of a CFST arch bridge to multi-component spatially varying ground motions. The 3D finite element model of the bridge is developed in ANSYS (2009), and the material and geometric nonlinearities of the concrete and the steel tube in the arch ribs are considered. The spatial variation of ground motions associated with the wave passage, coherency and local sit effects are considered. The base rock motions are assumed consisting of out-of-plane and in-plane waves and are modelled by a filtered Tajimi-Kanai power spectral density function and an empirical coherency loss function. Seismic waves then propagate vertically through local sites to ground surface. The 3D spatially varying ground motions at different supports of the bridge are then stochastically simulated based on the combined spectral representation method and the 1D wave propagation theory (Bi and Hao 2012). The influences of ground motion spatial variations and varying site conditions on the seismic responses of the CFST arch bridge are analyzed.

2. BRIDGE MODEL

2.1 Bridge description

The bridge to be investigated is the Yeshan River Bridge, which is a half-through CFST arch bridge in China. Fig. 2.1 shows the elevation and plan view of the bridge. The total length of the bridge is 138.65m with an arch span of 124m. Owing to the specific geological conditions of local sites, an asymmetric arc was selected. The length of the left half span (Yichang direction in Fig. 2.1(a)) is 70.375m with a rise at the crown of 40m, giving a rise-span ratio of 1: 3.52. For the right half span (Wanzhou direction in Fig. 2.1(a)), the length and rise are 53.625 and 24.15m respectively, and the rise-span ratio is 1: 4.44. Because of the asymmetric configuration of the bridge, the springing position of the right span is 15.85m higher than that of the left span. The width of the bridge is 15.3m. The bridge is located at a V-shape canyon site, the elevation difference between the bridge deck and the base rock is about 160m based on the geological report of the bridge.

The bridge has two parallel arch ribs, with the center-to-center distance of 13.1m as shown in Fig. 2.1(b). Each arch rib consists of two dumbbell-type cross section members (the upper chord and lower chord). These two members are connected by the H-type steel webs as shown in Fig. 2.2(a). The depth and width of each arch rib are 3.8 and 2.2m respectively. The four steel tubes of each arch rib have an outer diameter of 800mm and a thickness that varies depending on the position of the arch rib. High fluidity concrete fills the four steel tubes and the confined space between the steel plates of the upper and lower chords as shown in Fig. 2.2(a). The two parallel arch ribs are connected by 6 spatial cross-bracing systems and a horizontal stiffening girder as shown in Fig. 2.1(b). The deck system consists of 5 T beams with the height of 1.5m arranged longitudinally at a spacing of 2.14m. The T beams are connected by 15 transverse diaphragms with the height of 2m. Fig. 2.2(b) shows the cross section of the deck system. The main arch ribs and the deck system are connected vertically by 20 suspenders. Each suspender consists of 127 smaller steel wires each with a diameter of 5.5mm. On the left span of the bridge, two piers are designed to support the deck system, with pier 1 (P1) on the arch support and pier 2 (P2) supported by the arch ribs as shown in Fig. 2.1(a).

2.2. Finite element model

A three-dimensional (3D) FE model of the Yeshan River Bridge was developed in ANSYS (2009). The arch ribs, webs, lateral bracings, stiffening girder, the deck system and the piers are modelled using 3D beam elements (BEAM188) based on the actual cross-sectional properties. All suspenders are modeled as truss elements (LINK10). It should be noted that each CFST arch rib consists of the

steel tube and the infilled concrete, these two components are modeled separately but with sharing nodes in the model. In other words, two elements are included between every two nodes, with one element for the steel tube and another for the concrete. Regarding the boundary conditions, the springing positions of the arch ribs and the base of pier 1 (P1) are fixed in all degrees of freedom (DOFs). The deck system is simply supported, the three translational DOFs at each node of the left and right ends of the girder (A1 and A2 in Figs. 1 and 3) are fixed except the longitudinal translational DOFs at A2 are released. Fig. 2.3 shows the 3D FE model of the bridge.

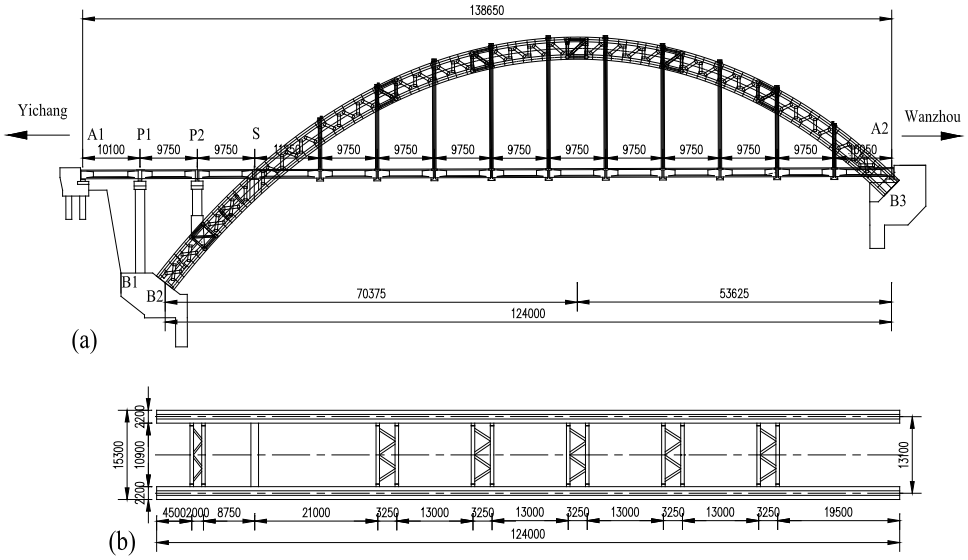

Figure 2.1. (a) Elevation view of the bridge, (b) plan view of the arch structure (unit: mm)

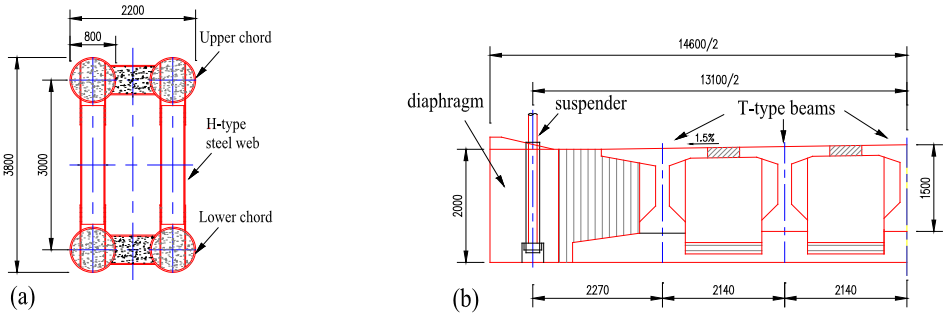

Figure 2.2. Cross sections of main bridge components (a) arch rib, (b) deck system (not to scale, unit: mm)

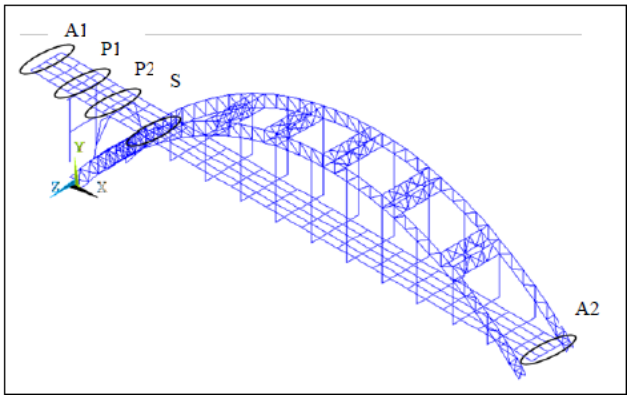

Figure 2.3. 3D FE model of Yeshan River Bridge

For long span structures, nonlinear analysis is essential to evaluate the stresses and deformations induced not only by static loads but also by dynamic loads. Both geometric and material nonlinearities are considered in the analysis. In ANSYS, the geometric nonlinearity can be conveniently considered by turn on the command NLGEOM (ANSYS 2009). The CFST arch ribs are the main load-bearing components of the bridge, only the material nonlinearities of the steel tube and the infilled concrete are considered. The elastic-perfect plastic model is usually suggested to consider the nonlinear behaviour of steel tube in many design codes such as JRA (2002), this model is adopted in the study. Fig. 2.4(a) shows the stress-strain curve of the steel tube, where σ_{sy} is the yield stress and is assumed to be 345 MPa. The stress-strain curve adopted by Wu *et al*. (2006), which takes into account the confinement of the infilled concrete, is used to model the material nonlinearity of the infilled concrete. Fig. 2.4(b) shows the curve, where σ_{cB} is the yield stress and ε_{cB} is the yield strain.

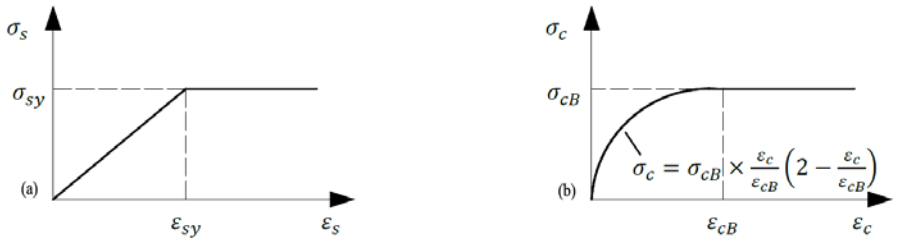

Figure 2.4. Stress-strain curves of the arch rib (a) steel tube, (b) concrete

With the detailed information mentioned above, the vibration frequencies and the corresponding vibration mode shapes of the bridge can be obtained by carrying out an eigenvalue analysis. It was found that the first three vibration modes of the bridge are in the transverse direction with the fundamental frequency of 0.6873Hz. Mode 4 is the first vertical mode with a frequency of 1.5931Hz and mode 7 is the first torsional mode with a frequency of 2.7429Hz.

3. SPATIALLY VARYING GROUND MOTIONS

The span length of Yeshan River Bridge reaches 138.65 m, the wave passage and coherency loss effect will inevitably result in the spatially varying ground motions. Furthermore, the Yeshan River Bridge is an asymmetric bridge with different elevations of different supports, the ground motion spatial variations are further intensified by local site effect. As shown in Fig. 2.1(a), Point B1 is close to B2 while B3 is next to A2, thus the ground motions at points B1 and B2 can be assumed to be the same. For the ground motions at points B3 and A2, the same assumption is made. Thus in this study, the spatially varying ground motions at three locations, i.e., at locations A1, B1/B2 and B3/A2, are simulated as inputs for bridge response analysis.

This paper simulated the spatially varying ground motions at different supports based on the method proposed by Bi and Hao (2012). In the method, the base rock motions are assumed to consist of out-of-plane SH wave and in-plane combined P and SV waves propagating into the site with an assumed incident angle. The power spectral density function on the base rock is assumed to be the same, and is modelled by a filtered Tajimi-Kanai power spectral density function. The spatial variation of ground motions at base rock is modelled by an empirical coherency function. Local site effect is modelled using the one-dimensional wave propagation theory. The power spectral density (PSD) functions of the horizontal in-plane, horizontal out-of-plane and vertical in-plane motions on the ground surface can thus be formulated by considering the site transfer functions in the corresponding directions. The 3D spatially varying ground motions can then be simulated by using the approach similar to the traditional method. This approach directly relates site amplification effect with local soil conditions, and can capture the multiple vibration modes of local site, is believed more realistically simulating the multi-component spatially varying motions on surface of a canyon site. More detailed information about the simulation technique can be found in Bi and Hao (2012).

To study the influence of different soil conditions, two different types of soil, namely firm and soft soil are considered. Table 3.1 shows the parameters for different soil conditions and base rock. It should be noted that, when an arch bridge is located at a relatively soft site, pile foundations are usually designed to resist the large axial force. In this case, the interaction between the structure and the surrounding soil (SSI effect) will further alter the structural responses. Not to further complicate the problem, the SSI effect is not considered in the present study even when soft soil is considered.

Table 3.1. Parameters for local site conditions

Type	Density (kg/m^3)	Shear modulus (MPa)	Damping ratio	Poisson's ratio
Base rock	2500	1800	0.05	0.33
Firm soil	2000	800	0.05	0.4
Soft soil	1800	200	0.05	0.4

Fig. 3.1 shows the simulated multi-component spatially varying acceleration time histories when firm soil is considered. Fig. 3.2 shows the comparisons of the simulated power spectral densities (PSDs) with the theoretical values of the horizontal out-of-plane motions, good agreements are observed. For conciseness, the comparisons of the in-plane motions are not plotted, good agreements are also observed. For the coherency loss function between the motions on the ground surface, Bi and Hao (2011) indicated that it is different from that on the base rock. The spatial ground motions on ground surface are least correlated when the spectral ratios of two local sites differ from each other significantly. Discussion of the influence of local soil condition on spatial ground motion coherency loss is out of the scope of the present study. More detailed information can be found in Bi and Hao (2011). It should be noted that when soft soil is considered, good agreement can also be observed.

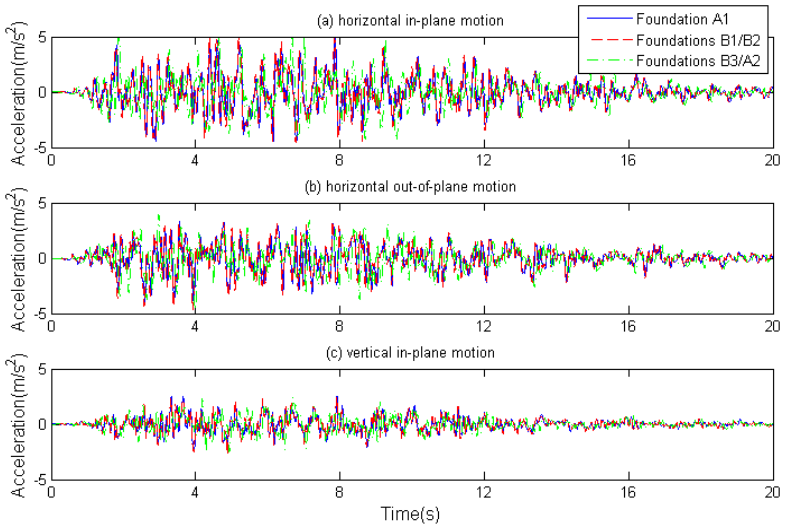

Figure 3.1. Simulated acceleration time histories with firm soil conditions

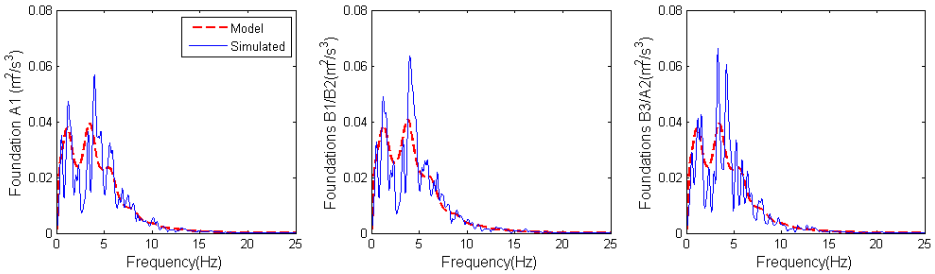

Figure 3.2. Comparisons of PSDs between the generated horizontal out-of-plane motions at different foundations with the respective theoretical values

4. EQUATIONS OF MOTION

To analyze the seismic response of large dimensional structures to spatially varying ground motions, two simple analytical methods are usually adopted. These are the relative motion method (RMM), which divides the structural response into a dynamic response component and a quasi-static response component, and the large mass method (LMM), which attributes fictitious large masses at each driven nodal DOFs to obtain the total response of the structure (Leger *et al*. 1990).

For large dimensional structure, the RMM might be very time consuming, since it requires an additional static solution at each time step used for the integration of the dynamic equilibrium equations. Also, it requires the integration of the input ground accelerogram to provide the ground displacement required for the static solution procedure. Moreover, the RMM cannot be directly extended to study the nonlinear responses of multi-support structures since the superposition is used. To overcome the limitations of RMM, the LMM is usually adopted to nonlinear seismic analysis of large dimensional structures to spatially varying ground motions.

The LMM was proposed by Leger *et al*. (1990). In order to specify the accelerations at the support DOFs, large masses (M_{ll}) are added at the driven support DOFs. To reproduce the specified accelerogram, the inertia forces developed at the supports should also be considered as external driving forces. In this case, the dynamic equilibrium equation can be written as (Leger *et al*. 1990)

$$\begin{bmatrix} M_{ss} & M_{sb} \\ M_{bs} & M_{bb}+M_{ll} \end{bmatrix} \begin{Bmatrix} \ddot{u}_s^t \\ \ddot{u}_b^t \end{Bmatrix} + \begin{bmatrix} C_{ss} & C_{sb} \\ C_{bs} & C_{bb} \end{bmatrix} \begin{Bmatrix} \dot{u}_s^t \\ \dot{u}_b^t \end{Bmatrix} + \begin{bmatrix} K_{ss} & K_{sb} \\ K_{bs} & K_{bb} \end{bmatrix} \begin{Bmatrix} u_s^t \\ u_b^t \end{Bmatrix} = \begin{Bmatrix} 0 \\ M_{bb}+M_{ll} \end{Bmatrix} \{\ddot{u}_g\} \tag{4.1}$$

where *[M]*, *[C]* and *[K]* are the mass, damping and stiffness matrices respectively, $\{\ddot{u}^t\}$, $\{\dot{u}^t\}$ and $\{u^t\}$ are the absolute acceleration, velocity and displacement vectors. $\{\ddot{u}_g\}$ is the corresponding spatially correlated free-field ground acceleration vector. The subscripts, *ss*, *bb* and *sb* denote the structural DOFs, the support DOFs and coupled DOFs, with *s* refers to the structure and *b* refers to the base. The second line of Eqn. 4.1 is

$$\begin{aligned} [M_{bs}]\{\ddot{u}_s^t\} + [M_{bb}+M_{ll}]\{\ddot{u}_b^t\} + [C_{bs}]\{\dot{u}_s^t\} + [C_{bb}]\{\dot{u}_b^t\} + [K_{bs}]\{u_s^t\} + [K_{bb}]\{u_b^t\} = \\ [M_{bb}+M_{ll}]\{\ddot{u}_g\} \end{aligned} \tag{4.2}$$

Since M_{ll} is much larger than other terms, the contribution of them thus can be neglected, which results in

$$\{\ddot{u}_b^t\} \approx \{\ddot{u}_g\} \tag{4.3}$$

The structural response is thus

$$\begin{aligned} [M_{ss}]\{\ddot{u}_s^t\} + [C_{ss}]\{\dot{u}_s^t\} + [K_{ss}]\{u_s^t\} &= -[M_{sb}]\{\ddot{u}_b^t\} - [C_{sb}]\{\dot{u}_b^t\} - [K_{sb}]\{u_b^t\} \\ &\approx -[M_{sb}]\{\ddot{u}_g\} - [C_{sb}]\{\dot{u}_g\} - [K_{sb}]\{u_g\} \end{aligned} \tag{4.4}$$

By setting the large mass M_{ll} equals to about 10^7 times the total mass of the bridge, it was found that LMM is able to yield results that are almost identical to those from RMM (Leger *et al*. 1990). The accuracy of LMM was thus validated.

The LMM can be conveniently implemented in ANSYS. The large masses are applied at the supporting nodes of the bridge (locations A1, A2, B1, B2 and B3 in Fig. 1) by using the MASS21 element in ANSYS and the value is 10^7 times the total mass of the bridge as suggested by Leger *et al*.

(1990). The seismic excitations are applied as external forces at different driven supporting nodes, and the values equal to the large masses multiplying the corresponding accelerations at different supports.

5. NUMERICAL RESULTS

The nonlinear seismic response of Yeshan River Bridge is investigated in this section. All the calculations are carried out by using the finite element code ANSYS. Rayleigh damping is assumed in the model to simulate energy dissipation during structural vibrations. The first two vibration modes are chosen to determine the mass and stiffness coefficients. By assuming the structural damping ratio of 5%, the mass matrix multiplier is obtained as 0.2537 and the stiffness matrix multiplier is 0.0096. To obtain relatively unbiased seismic responses of the structure, independent numerical calculations are performed by using three sets of independently simulated spatial ground motions as inputs. The mean peak responses, which are mostly concerned in engineering practice, are calculated and discussed.

5.1. Effect of ground motion spatial variations

To study the influence of ground motion spatial variations on Yeshan River Bridge, following three cases are considered. Particularly, Case 1 corresponds to uniform ground motions, Case 2 considers spatial ground motions with wave passage effect only, and Case 3 is a general case which considers spatial ground motions with both wave passage effect and coherency loss effect. Therefore, the significance of ground motion spatial variations increases from Case 1 to Case 3. In the study, the bridge is assumed at a firm site and 3D excitations are considered.

Fig. 5.1 shows the axial forces in the arch ribs when the bridge is subjected to different spatially varying ground motions. With uniform excitations (Case 1), the responses are almost symmetric, since uniform ground motions excite only the symmetric modes. When spatially varying ground motions are considered, the asymmetric vibration modes will be excited, and the contribution of asymmetric vibration modes are especially significant at the middle span of the bridge. Taking the minimum axial force at the arch span of 59m of the upper chord as the example, the values are -10900, -15200 and -18700kN respectively for the three different cases. Uniform ground motions will significantly underestimate the axial forces in the arch ribs. Considering spatial ground motion wave passage effect (Case 2) results in slightly smaller responses than the general case (Case 3). These results, on the other hand, indicate that the contribution of coherency loss effect is relatively small compared with the wave passage effect for Yeshan River Bridge. This is because as indicated in a previous study (Hao 1993), spatial ground motion wave passage effect is more significant if the structure is relatively flexible and spatial ground motion coherency loss effect becomes more pronounced if the structure is relatively stiff. The fundamental vibration frequency of Yeshan River Bridge is 0.6873Hz as mentioned above, which is a relatively flexible structure. Therefore, the ground motion wave passage effect is more significant than coherency loss effect.

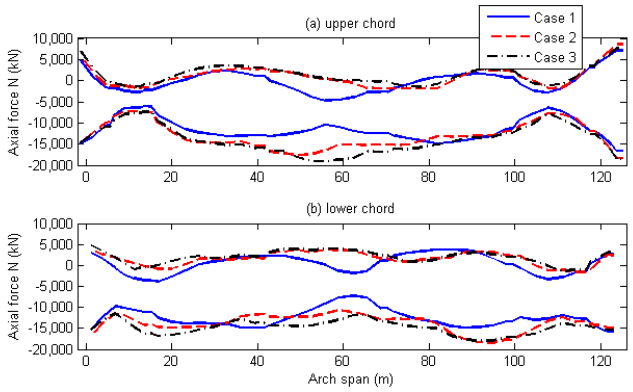

Figure 5.1. Influence of ground motion spatial variations on the axial force N

Figs. 5.2 and 5.3 show the influence of ground motion spatial variations on the in-plane bending moment Mz and out-of-plane bending moment My. Contrast with the axial force, the influence of ground motion spatial variations on the bending moments is relatively less and can be neglected, and uniform excitations can give a good prediction of the bending moments.

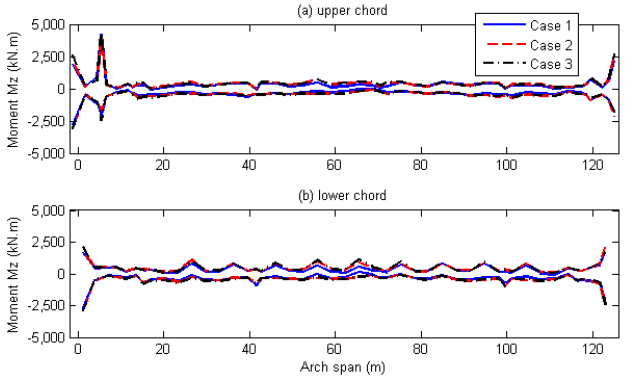

Figure 5.2. Influence of ground motion spatial variations on the in-plane bending moment Mz

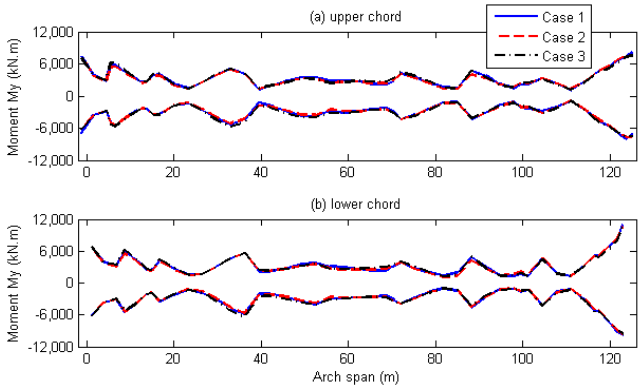

Figure 5.3. Influence of ground motion spatial variations on the out-of-plane bending moment My

5.2. Effect of local soil conditions

Yeshan River Bridge is located at a canyon site as mentioned above, local soil conditions may have important influence on the seismic responses because of the site filtering and amplification effect on the ground motions. To study the influence of local site effect, three different cases are considered. Cases 3 and 4 assumed that the soil conditions under different supports are the same with Case 3 considering firm soil and Case 4 considering soft soil. Case 5 assumed the soil conditions of the canyon are different, with supports A1 and B1/B2 located at a soft site and B3/A2 at firm site. For all the three cases, 3D spatially varying ground motions are considered and for each case the same coherency loss and apparent wave velocity are assumed, the only difference between them is the site conditions.

Fig. 5.4 shows the influence of local soil conditions on the axial forces N. As shown, site conditions substantially affect the axial forces of the arch ribs. When the bridge is located at a homogeneous site (Cases 3 and 4) with softer soil conditions, larger axial forces areobtained. This is because softer soil leads to larger displacement at different supports of the bridge (Bi and Hao 2012), which in turn gives rise to larger structural responses. When the bridge is located at a heterogeneous site (Case 5), the axial forces are the largest among the three cases, which indicates the significant effect of ground motion spatial variations. Because Case 5 corresponds to a heterogeneous soil conditions, the ground displacements are between those of the firm soil and soft soil, however, Case 5 ground motions induce

the largest axial forces, indicating the significant effect of ground motion spatial variations. Neglecting the varying soil conditions on ground motion spatial variations may substantially underestimate the axial forces in the arch ribs. Fig. 5.5 shows the influence of local soil condition on the envelopes of in-plane bending moments Mz in the upper and lower chords of the arch rib. As shown, three soil conditions result in almost the same in-plane bending moment Mz except at the springing positions, where heterogeneous soil conditions lead to relatively larger Mz. Fig. 5.6 shows the envelopes of out-of-plane bending moments My. As shown, My from the Case 4 ground motions are the largest and those from Case 3 are the smallest. This is because softer soil conditions result in larger displacements at the bridge supports as mentioned above. These observations indicate that the out-of-plane bending moments My strongly depend on the ground motion displacement, ground motion spatial variation has a relatively less effect on My.

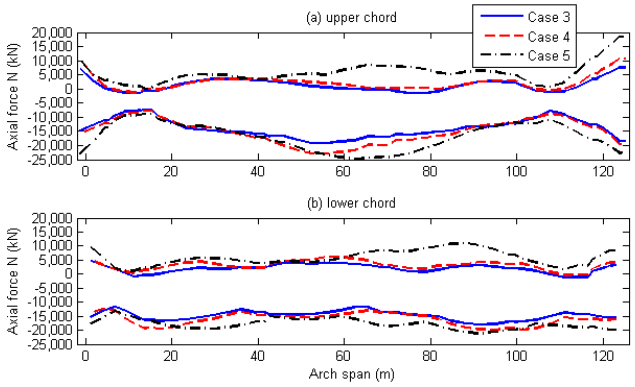

Figure 5.4. Influence of local soil conditions on the axial force N

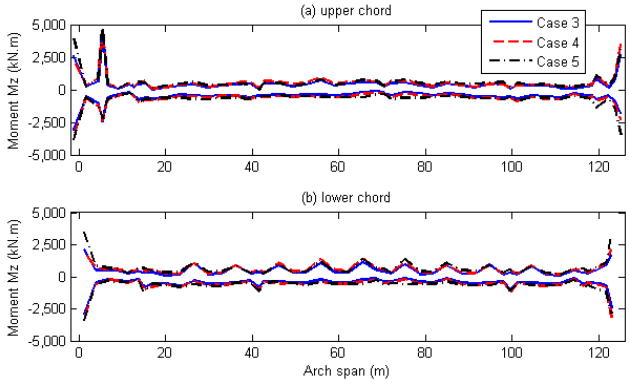

Figure 5.5. Influence of local soil conditions on the in-plane bending moment Mz

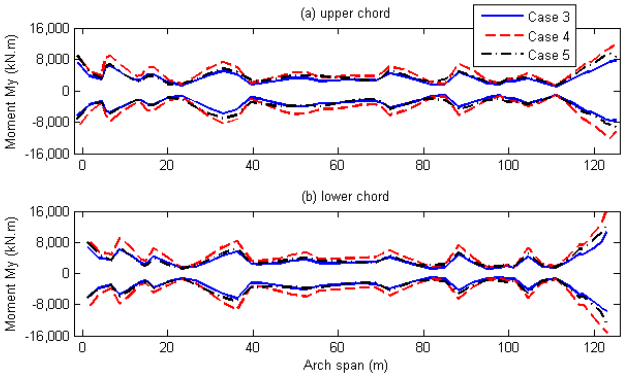

Figure 5.6. Influence of local soil conditions on the out-of-plane bending moment My

CONCLUSIONS

This paper studies the nonlinear seismic responses of a CFST arch bridge to multi-component spatially varying ground motions. The 3D finite element model of the CFST arch bridge is developed with consideration of the material and geometric nonlinearities of the arch ribs. The spatial variation of ground motions associated with wave passage, coherency loss and local site effects are considered. The influences of ground motion spatial variations and varying site conditions on the seismic responses of the CFST arch bridge are analysed. Following conclusions are obtained:

(1) The influence of ground motion spatial variations has significant influence on the axial forces of CFST arch bridge. Neglecting ground motion spatial variations may significantly underestimate the axial forces in the arch ribs. The influence of wave passage effect is more evident than coherency loss effect for Yeshan River Bridge.

(2) The influence of ground motion spatial variations on the bending moments of Yeshan River Bridge can be neglected.

(3) Ground motion spatial variations induced by local site effect have significant influence on structural response. Heterogeneous local soil conditions result in largest axial forces in the arch ribs. Bending moments are sensitive to the ground motion displacement, larger ground motion displacements lead to larger bending moments in the structure.

ACKNOWLEDGEMENT

The authors acknowledge the partial financial support from ARC Linkage project LP110200906 for carrying out this research.

REFERENCES

ANSYS. ANSYS user's manual revision 12.1. (2009). ANSYS Inc.

Bai, F., Hao, H. and Li, H. (2010). Seismic response of a steel trussed arch structure to spatially varying earthquake ground motions including site effect. *Advances in Structural Engineering* **13:6**, 1089-1103.

Bi, K. and Hao, H. (2011). Influence of irregular topography and random soil properties on coherency loss of spatial seismic ground motions. *Earthquake Engineering and Structural Dynamics* **40:9**, 1045-1061.

Bi, K. and Hao, H. (2012). Modelling and simulation of spatially varying earthquake ground motions at sites with varying conditions. *Probabilistic Engineering Mechanics* **29**, 92-104.

Der Kiureghian, A. (1996). A coherency model for spatially varying ground motions. *Earthquake Engineering and Structural Dynamics* **25:1**, 99-111.

Hao, H. (1993). Arch response to correlated multiple excitations. *Earthquake Engineering and Structural Dynamics* **22:5**, 389-404.

Hao, H. (1995). Ground motion spatial variation effects on circular arch responses. *Journal of Engineering Mechanics* **120:11**, 2326-2341.

Harichandran, R.S., Hawwari, A. and Sweiden B.N. (1996). Response of long-span bridges to spatially varying ground motion. *Journal of Structural Engineering* **112:5**,476-484.

Japan Road Association. (2002). Design specifications for highway bridges, part V: Seismic design.

Leger, P., Ide, I.M. and Paultre, P. (1990). Multiple-support seismic analysis of large structures. *Computers and Structures* **36:6**, 1153–1158.

Su, L., Dong, S.L. and Kato, S. (2007). Seismic design for steel trussed arch to multi-support excitations. *Journal of Constructional Steel Research* **63:6**, 725-734.

Wu, Q., Yoshimura, M., Takahashi, K., Nakamura, S. and Nakamura T. (2006). Nonlinear seismic properties of the Second Saikai Bridge: A concrete filled tubular (CFT) arch bridge. *Engineering Structures* **28:2**, 163-182.

Zanardo, G., Pellegrino, C., Bobisut, C. and Modena, C. (2004). Performance evaluation of short span reinforced concrete arch bridges. *Journal of Bridge Engineering* **9:5**, 424-434.